VOL. 13, NO. 1, JANUARY 2018 ISSN 1819-6608
ARPN Journal of Engineering and Applied Sciences

www.arpnjournals.com

# A MATHEMATICAL MODEL TO STUDY THE PROPAGATION OF PITTING CORROSION IN STEEL IMMERSED IN CHLORIDE SOLUTION

Suhaila Salleh[1, 2] and Nicholas P. C. Stevens[3]
[1]Faculty of Mechanical Engineering, Universiti Teknikal Malaysia Melaka, Hang Tuah Jaya, Durian Tunggal, Melaka, Malaysia
[2]Centre for Advanced Research on Energy, Universiti Teknikal Malaysia Melaka, Hang Tuah Jaya, Durian Tunggal, Melaka, Malaysia
[3]Materials Performance Centre, University of Manchester, Manchester M13 9PL, United Kingdom
E-Mail: suhaila@utem.edu.my

**ABSTRACT**

This paper presents the mathematical model of the propagation of pitting corrosion using a commercial finite element program, COMSOL Multiphysics. In view of the chemical and electrochemical reactions inside a single pit in steel, a two dimensional model that allows the prediction of pit evolution is developed. The model is solved under the Nernst-Planck resolution. The results show that different sites of the geometry give different current densities and different concentrations of ionic species. In addition, the pH inside the corroding pit is also shown to reduce gradually as hydrogen ions gradually accumulate inside the pit, an occurrence expected in pitting behaviour.

**Keywords:** pitting corrosion, model, steel, simulation.

## INTRODUCTION

Pitting is a highly destructive formed of localized corrosion. It is regarded as the most hazardous type of corrosion and has the tendency to undercut the metal surface through the formation of small cavities on a metal surface. The mass of the metal loss is less compared to uniform corrosion and the bulk of the metal surface remains unattacked. The formation of corrosion pits can be difficult to detect given that they have the tendency to undercut the metal surface and is usually covered by corrosion residue. Not only that, pits may occur in isolated sites or be so intense in their formation that it looks like uniform attack. As a result, metals subjected to corrosion pits may loss their properties and thus, affect the structural integrity of much equipment. (Fontana 1987; Shreir 2000; Shreir 2000; Perez 2004; Ahmad 2006).

Corrosion is basically the result of interaction between materials and their environment (Ahmad 2006). (Ergun 2002) and (Papavinasam 2010) stated that corrosive environments include the existence of factors such as air and humidity, water (e.g. fresh, salt, marine, distilled), hydrogen sulphide (which is common in marine environment), acids, alkalis, etc. (Cui 2001) stated that pitting is induced by the presence of halides, such as chlorides or bromides, whereas (Cheng 2000) stated that pitting frequently occurs in situations where general corrosion is prevented by passive oxide film that forms on the surface of metal. Once broken down, the metal surface is liable to corrosion attack. However, it has the ability to self-repair and thus, remains as passive metal. Corrosion sites that are not able to repair itself are liable for localized corrosion to occur. With the presence of halides, rigorous corrosion occurs. It is, however, established that the pH inside a pit drops to a value way below the pH of the bulk solution. Furthermore, it is also established that there are three stages of pitting (Burstein 1993; Laycock 2001; Perez 2004; Ahmad 2006): (i) initiation of pits, (ii) formation of metastable pits and (iii) stable pitting. These stages of pitting are controlled by the ability of metal to be in active to passive condition, and vice-versa. Hence, in order to understand the stages of pitting, one needs to understand the active/passive transition of metal.

Carbon steel is known susceptible to pitting corrosion, given that it is in slightly alkaline conditions, as stated by (Alvarez 1984) and (Fushimi 2006). On the other hand, stainless steel is less susceptible to corrosion, but it is more expensive. However, common stainless steels are also susceptible to pitting corrosion in aqueous chloride conditions (Schmuki 1992). To understand pitting corrosion in steel, many modelling work have been published. (Salleh and Stevens 2012) modelled the corrosion activities at neutral environment of pH7 with the presence of chloride, and the results show a drop in potential and pH at corroding sites. Therefore, it is published that pitting corrosion occurs in iron-based metal depending on its environmental conditions. For that reason, this research studies the occurrences of pitting corrosion in iron-based metal.

Over the years, there is an extensive literature on the modelling of pit propagation. (De Meo and Oterkus 2017) and (Salleh 2013) modelled the evolution of pitting corrosion and predict the pit shape by considering mathematical formulation based on a simplified version of the Nernst-Planck equation. Nonetheless, the novelty of this study is the model construction which focuses on the electrochemistry of ionic species during pitting and also the unique incorporation of the mathematical rules to predict pitting behaviour. COMSOL Multiphysics version 4.2 is used as tool to run the results.

## METHODOLOGY

This model is developed to look at the propagation of a single pit, corroding stably, in steel immersed in aqueous sodium chloride solution. (Salleh 2013) constructed two-dimensional axial symmetry geometry to represent a micropit and considered thirteen

neutral aqueous chemical species. This study looks at eleven species to illustrate the corrosion model ($Fe^{2+}$, $OH^-$, $H^+$, $FeOH^+$, $Na^+$, $Cl^-$, $FeCl^+$, $H_2$, $Fe^{3+}$, $FeO_2^-$, $HFeO_2^-$). The behaviour of these ionic species is governed by the Nernst-Planck law for the case where electroneutrality is enforced (Turnbull 1982; Sharland 1988; Perez 2004):

$$\frac{\partial[i]}{\partial t} = D_i \nabla^2 [i] + z_i U_i F \nabla([i] \nabla V) + R_i \quad (1)$$

where $[i]$ - concentration of species $i$, $D_i$ - effective diffusion coefficient, $z_i$ - charge number, $U_i$ - mobility (given that $U_i = \frac{D_i}{RT}$), $R_i$ - rate of production/depletion of $i$, $\nabla V$ - potential gradient.

To counter for the active state of metal, the model studies the respective currents for metal dissolution and reduction of hydrogen ions, $H^+$, which applies Tafel expression (Turnbull 1982; Turnbull 1982; Galvele 2005). Hence, the current densities for both iron oxidation, $i_1$, and proton reduction, $i_2$, are, respectively, given as:

$$i_1 = i_{01} \exp\left[ a_1 F \frac{(V_m - V)}{RT} \right] \quad (2)$$

$$i_2 = i_{02} [\mathrm{H}^+] \exp\left[ a_2 F \frac{(V_m - V)}{RT} \right] \quad (3)$$

where $V_m$ is the metal potential, $V$ is the electrostatic potential in solution, $[H^+]$ is the concentration of $H^+$, $a_1$ and $a_2$ are the rate constants.

The metal dissolution rate and the hydrogen ions reduction rate follow Fick's First Law of Diffusion (Smith 2006) which stated that the kinetics in Equations (2) and (3) produce their respective fluxes (Turnbull 1987), as stated below. The predicted concentration and potential distributions are determined by ionic fluxes, as stated in Equation (4) and (5) below.

Flux of metal ions $Fe^{2+}$ (dissolution rate):

$$J_{diss} = \frac{i_1}{2F} = \frac{0.25 \times i_{01}}{F} \exp\left[ a_1 F \frac{(V_m - V)}{RT} \right] \quad (4)$$

Flux of hydrogen ions $H^+$ (reduction rate):

$$J_{H^+} = -\frac{i_2}{F} = \frac{i_{02} \times [\mathrm{H}^+]}{F} \exp\left[ a_2 F \frac{(V_m - V)}{RT} \right] \quad (5)$$

where $i_{01} = 2.7 \times 10^{11}$ A m$^{-2}$, $i_{02} = 2 \times 10^7$ A m mol$^{-1}$, $a_1 = 1$ and $a_2 = 0.5$. (Vuillemin 2007).

A change in pH level can also be observed once corrosion is initiated. The pH is calculated by the concentration level of hydrogen ion, $H^+$ and stated as Equation (6) below:

$$\mathrm{pH} = -\log_{10}(0.001 \times \mathrm{abs}[\mathrm{H}^+]) \quad (6)$$

Meanwhile, to find the production and depletion rate of ionic species, (Sharland and Tasker 1988) applied the law of equilibrium. Having calculated the rates, the mass transport equations for each species can then be determined. COMSOL Multiphysics 4.2 runs the model under the environment of pH 8 and applying the initial concentration of chloride concentration to be 500 mol per cubic meter. By considering chloride concentration, pH calculation and potential, a function is introduced which applies the line construction of a theoretical Pourbaix diagram. These functions distinguish the region of corrosion and passivity and applied the Nernst equation, which is:

$$E = E^0 + \frac{0.059}{z} \log\left( \frac{\text{product of activities of oxidation}}{\text{product of activities of reduction}} \right) \quad (7)$$

Given that $\mathrm{pH} = -\log_{10}[\mathrm{H}^+]$, substituting in Equation (7) above gives:

$$E = E^0 - 0.059 \frac{m}{z} \mathrm{pH} - \frac{0.059}{z} \log \frac{\text{product of activities of oxidation}}{\text{product of activities of reduction}} \quad (8)$$

where $m$ is the number of $H^+$ used and $z$ is the number of electrons transferred in the reaction.

## RESULTS AND DISCUSSIONS

The geometry of the model is an axial two-dimensional model, as shown in Figure 1. Points 1 and 5-8 are points in active regions whilst Points 2, 3 and 9 are indicated as inactive points. The rest are indicated as in neutral state. The regions set as active boundaries are where metal dissolution occurs. The model is solved in Nernst-Planck mode for a variety of potential range.

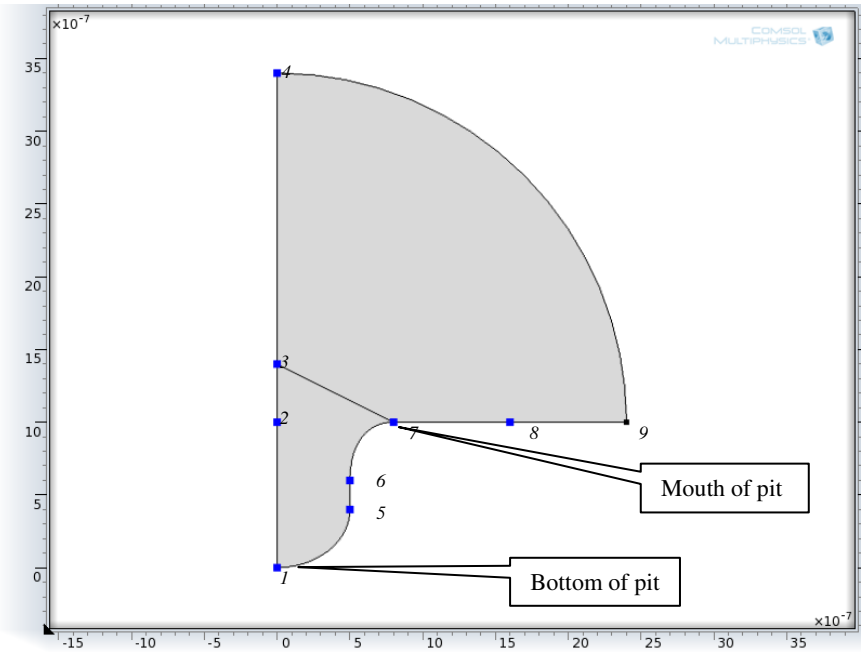


**Figure-1.** Geometry representing an axial-symmetry single pit with curved bottom and narrow mouth with 9 points of interest.

The polarization curve in Figure-2 below shows that at potential -0.74 V, the potential start to increase. It can be concluded that metal dissolution starts to occur and -0.74 V and is the corrosion potential of the system. Relating to Pourbaix diagram, this is where the metal changes from passive/immune state to active/corroding state. The corrosion rate is also seen to have different rates above -0.45 V. It can be concluded that metal dissolution occurring at different rates and may contribute to the different shapes of pit. From the graph, the current density is higher at Point 7 and 8, which are situated outside the pit, compared to the points inside the pit (Point 1, 5 and 6. This is supported by (Vuillemin 2007) who indicates that the saturation of metal ions inside a pit results in lower corrosion rate. This, as a result, causes reduction of outward diffusion of metal ions into the bulk solution.

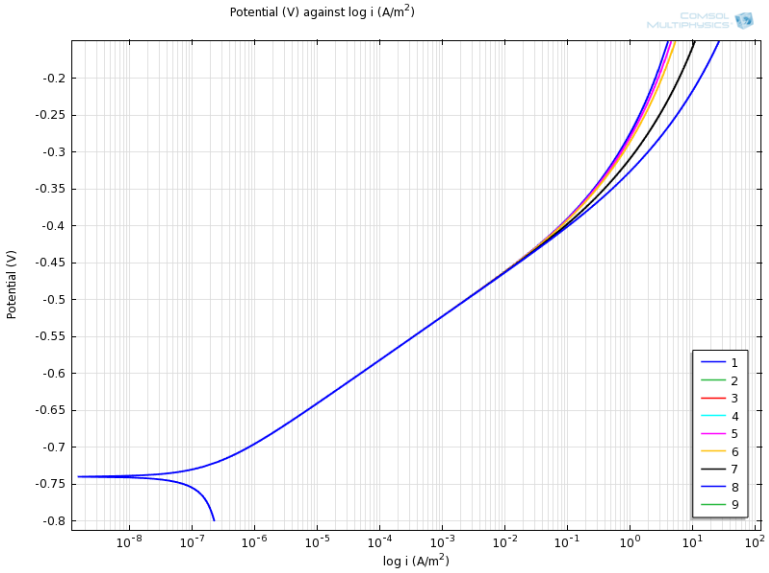


**Figure-2.** The polarization curve at Points 1-9 solve at potential range [-0.8,-0.1] V.

At the earlier stage, the model shows corroding activities continuing throughout all the active boundaries. From Figure-2, it can also be seen that from around -0.35V, the slope of the current density starts to decrease. Nevertheless, the current density still maintains at a high level, indicating the occurrence of corrosion activities. Referring to Figure-3 below, the points inside the pit (Points 1, 5 and 6) are seen to have higher concentration of

$Fe^{2+}$ at potential less than -0.2V compared to the points outside the pit (Points 7 and 8). However, at above -0.2V the accumulation of Fe2+ inside the pit is seen to have reduced. It is concluded that this may be due to the saturated concentration of ionic species inside the pit.

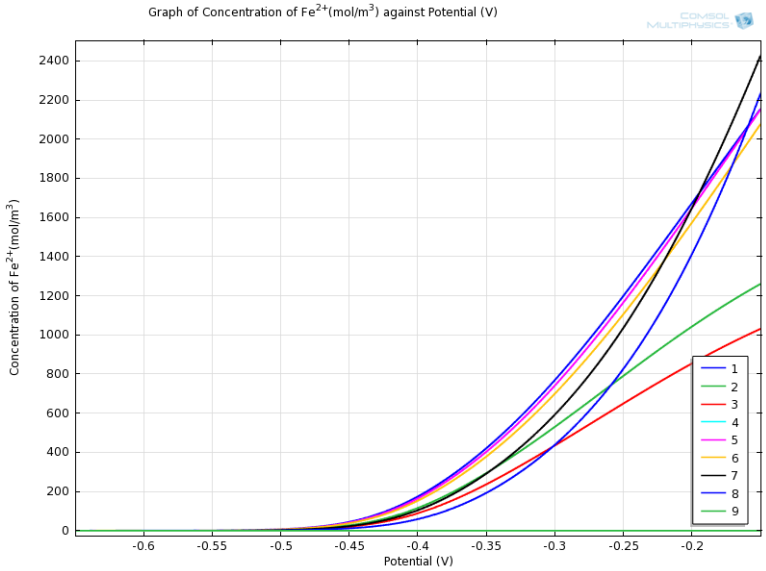


**Figure-3.** Concentration levels of $Fe^{2+}$ at different region.

The higher concentration of $Fe^{2+}$ outside the pit is also seen in Figure-4 below. Relating to Figure-3 above, at potential less that -0.2 V, the $Fe^{2+}$ concentration at the bottom of the pit is at the highest level, indicating that metal dissolution rate is highest at this stage. However, above -0.2 V, the concentration level of $Fe^{2+}$ is higher at the mouth of the pit. This may indicate that the pit shape is more of open-mouthed or dish-shaped, rather than trough-like. The predicted dish-shaped geometry is supported by the work done by (Moayed 2006).

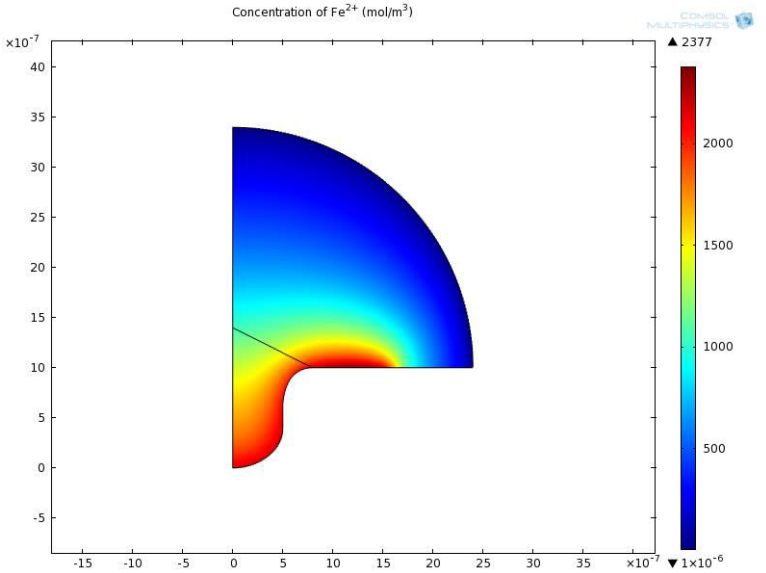


**Figure-4.** Concentration distribution of $Fe^{2+}$ after 600 seconds.

The increase in current density indicates the occurence of corrosion activities. Accumulation of $H^+$ is expected at the corroding region and hence, reduces the pH of that particular region. From Figure-5 below, simultaneous reaction to the production of $Fe^{2+}$ causes $H^+$ to also accumulate inside the pit, creating a positively charged environment. Therefore, this phenomenon attracts negatively charged species into the pit, in particular, $Cl^-$, and producing acid hydrocholric acid, HCl. The pH at the bottom of the pit reduces to about 4.9, as shown in Figure-6. This is supported by (Lee 1981) and Mankowski and (Mankowski 1975) who also stated that this acidic environment lowers the pH inside pit.

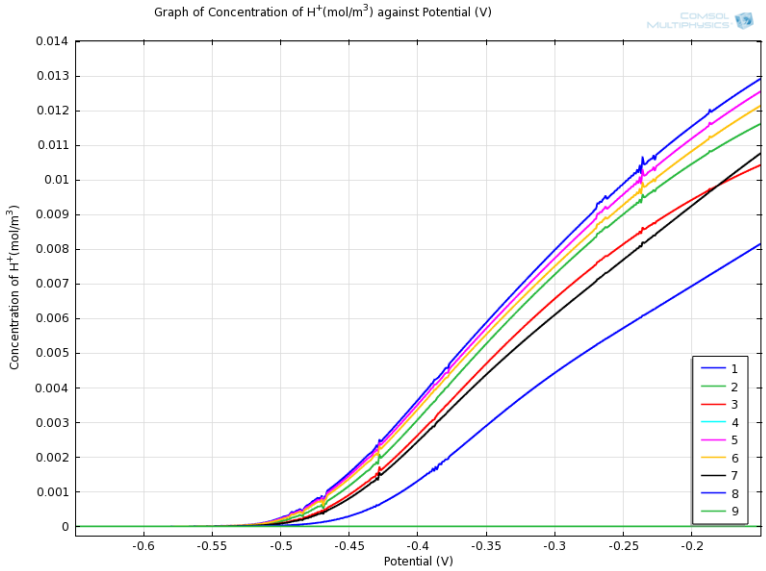


**Figure-5.** Concentration levels of $H^+$ at different region

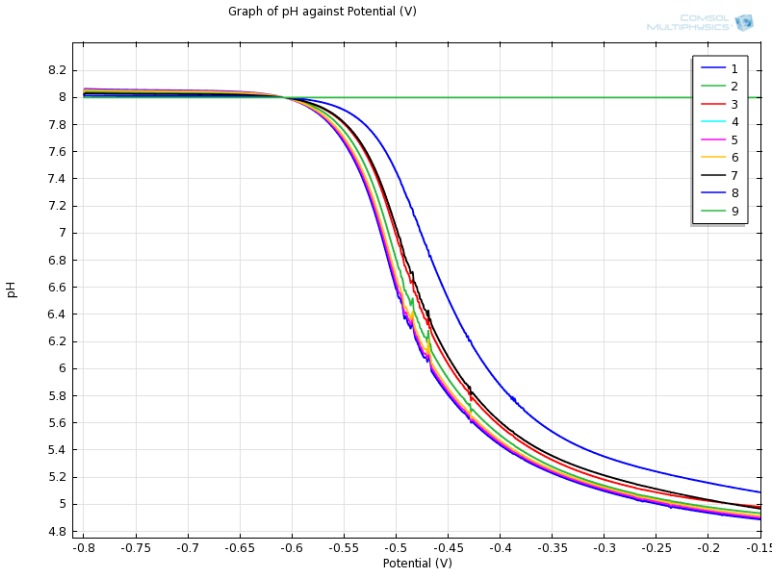


**Figure-6.** pH at different locations of the pit.

## CONCLUSIONS

As a conclusion, the model is able to produce similar results to published study, in particular the ascending pattern in current densities, the increasing concentration levels of ionic metal, particularly $Fe^{2+}$, indicating the occurrence of metal dissolution and the change in pH inside the pit geometry. This concludes that the model is able to integrate the electrochemistry and mass transport reactions involved in corrosion activities and will be able to portray further pitting behaviour in future work.

## ACKNOWLEDGEMENTS

This work was supported by the Ministry of Higher Education of Malaysia and the Universiti Teknikal Malaysia Melaka.

## REFERENCES

Ahmad Z. 2006. Principles of Corrosion Engineering and Corrosion Control, Butterworth-Heinemann.

Alvarez, M. G., Galvele, J.R. 1984. The mechanism of pitting of high purity iron in NaCl solutions. Corrosion Science. 24(1): 27-48.

Burstein G. T., Pistorius P.C. and Mattin S.P. 1993. The nucleation and growth of corrosion pits on stainless steel. Corrosion Science. 35(1-4): 57-62.

Cheng Y. F., Luo J.L. 2000. A comparison of the pitting susceptibility and semiconducting properties of the passive films on carbon steel in chromate and bicarbonate solutions. Applied Surface Science. 167: 113-121.

Cui, N., Ma, H.Y., Luo, J.L., and Chiovelli S. 2001. Use of general reference electrode technique for characterizing pitting and general corrosion of carbon steel in neutral media. Electrochemistry Communications. 3: 716-721.

De Meo, D. and E. Oterkus. 2017. Finite element implementation of a peridynamic pitting corrosion damage model. Ocean Engineering. 135: 76-83.

Ergun M., Akcay L. 2002. Investigation of pitting potential of carbon steel using experimental design method. British Corrosion Journal. 37(3): 235-238.

Fontana M. G. 1987. Corrosion Engineering. Singapore, McGraw-Hill.

Fushimi K., Takase K., Azumi K. and Seo M. 2006. Current transient of passive iron observed during micro-indentation in pH 8.4 borate buffer solution. Electrochemica Acta. 51: 1255-1263.

Galvele J. R. 2005. Tafel's law in pitting corrosion and crevice corrosion susceptibility. Corrosion Science. 47: 3053-3067.

Laycock N. J. and White S.P. 2001. Computer simulation of single pit propagation in stainless steel under potentiostatic control. Journal of the Electrochemistry Society. 148(7): B264-B275.

Lee Y. H., Takehara Z. and Yoshizawa S. 1981. The enrichment of hydrogen and chloride ions in the crevice corrosion of steels. Corrosion Science. 21(5): 391-397.

Mankowski J., Szklarska-Smialowska Z. 1975. Studies on accumlation of chloride ions in pits growing during anodica polarization. corrosion Science. 15: 493-501.

Moayed M. H., Newman R.C. 2006. The relationship between pit chemistry and pit geomwtry near the critical pitting temperature. Journal of Electrochemical Society. 153(8): B330-B335.

Papavinasam S., Doiron A., Li J., Park D. and Liu P. 2010. Sour and sweet corrosion of carbon steel: General or pitting or localized or all of the above? NACE Corrosion 2010.

Perez N. 2004. Electrochemistry and Corrosion Science. United States of America, Kluwer Academic Publisher.

Salleh S. 2013. Modelling pitting corrosion in carbon steel materials, The University of Manchester, Manchester, UK.

Salleh S. and N. Stevens. 2012. A Theoretical Model of Pitting Corrosion Using a General Purpose Finite Element Package. Journal of Mechanical Engineering and Technology (JMET) 4(1).

Schmuki P., Bohni H. 1992. Metastable pitting and semiconductive properties of passive film. Journal of Electrochemical Society. 139(7): 1908-1913.

Sharland S. and P. Tasker. 1988. A mathematical model of crevice and pitting corrosion-I. The physical model." Corrosion Science 28(6): 603-620.

Sharland S. M. 1988. A mathematical model of crevice and pitting corrosion - II. The mathematical solution. Corrosion Science 28(6): 621-630.

Shreir L. L. e. a. 2000. Corrosion: Corrosion Control, Butterworth-Heinemann.

Shreir L. L. e. a. 2000. Corrosion: Metal/Environment Reactions, Butterworth-Heinemann.

Smith W. F. and Hashemi J. 2006. Foundations of Materials Science and Engineering. Singapore, McGraw-Hill.

Turnbull A. 1987. Mathematical modelling of the electrochemistry in corrosion fatigue cracks in steel corroding in marine environments. Corrosion Science. 27(12): 1323-1350.

Turnbull A. and Gardner M.K. 1982. Electrochemical polarization studies of BS 4360 50D steel in 3.5% NaCl. Corrosion Science. 22(7): 661-673.

Turnbull A. and Thomas J.G.N. 1982. A model of crack electrochemistry for steels in the active state based on mass transport by diffusion and ion migration. Journal of Electrochemical Society. 129(7): 1412-1422.

Vuillemin B., Oltra R., Cottis R. and Crusset, D. 2007. Consideration of the formation of solids and gases in steady state modelling of crevice corrosion propagation. Electrochemica Acta. 52: 7570-7576.